# Quasi-periodic Motions of a Rigid Body I

## Quadratic Hamiltonians on the Sphere with a Distinguished Parameter

Heinz Hanßmann

*Institut für Reine und Angewandte Mathematik der RWTH Aachen*
*52056 Aachen, Germany*

12 Mai 1997

**Abstract**

The motion of a dynamically symmetric rigid body, fixed at one point and subject to an affine (constant+linear) force field is studied. The force being weak, the system is treated as a perturbation of the Euler top, a superintegrable system. Averaging along the invariant 2-tori of the Euler top yields a normal form which can be reduced to one degree of freedom, parametrised by the corresponding actions. The behaviour of this family is used to identify quasi-periodic motions of the rigid body with two or three independent frequencies.

## Introduction

The general motion of a free rigid body is quasi-periodic, being a combination of precession and rotation. The corresponding trajectories of the equations of motion lie dense on invariant 2-tori. The present work originated from the question *"What happens to these Eulerian 2-tori under perturbation by a weak external force field ?"*

Among all problems of rigid body dynamics, the most studied one is certainly that of a *heavy rigid body*, *i.e.* subject to a constant gravity. In such a case the system is invariant under an $S^1$-action, generated by the rotations about the direction of the force. Consequently the system admits a second integral of motion, besides energy, namely the projection of the angular momentum along the direction of gravity, the so-called *area-integral*. This can be used to solve the above problem in the special case of constant forces, confer [Arnol'd;63a]. Indeed, fixing the value of the area integral and dividing the $S^1$-symmetry we reduce the number of degrees of freedom from 3 to 2 . In the reduced system the Eulerian 2-tori become maximal tori, and KAM-theory tells us that most of these survive a small perturbation. However, the reconstructed motion in three degrees of freedom is quasi-periodic with three frequencies, the fast precessional-rotational motion about the angular momentum being superposed by a slow precession of the angular momentum about the direction of gravity. Only for angular momenta parallel to the constant force we obtain surviving Eulerian 2-tori.

In case the force field does not admit a rotational symmetry one has to proceed differently ; in fact this is exactly the situation we are interested in. We will work with *affine force fields*, *i.e.* with force fields that are the sum of a constant force and a linear force field. When the coefficients of the linear part are in general position, the rotational symmetry of the constant part is destroyed. Affine force fields are appealing in that they do not involve moments of the mass distribution other than the well-known centre of mass and the three principal moments of inertia. One might also think of the affine force field as the truncation of the Taylor series of a "general" force field. However, if a concrete force field is given, one does not have to resort to its affine truncation but can apply directly the techniques laid out here. The occurrence of discrete symmetries may equally influence the motion of the rigid body. In [Hanßmann;96] a case is studied where the external force field admits a $\mathbb{Z}_2 \times \mathbb{Z}_2$-symmetry. The methods we will use also apply in this situation, with easier computations that allow for explicit expressions.

Recall that a nondegenerate integrable Hamiltonian system $X_H$ with 3 degrees of freedom has three-parameter families of invariant 3-tori, two-parameter families of invariant 2-tori, one-parameter families of periodic orbits and isolated equilibria. We say that the phase space becomes a *ramified* 3*-torus bundle*. If we study a single system that is a sufficiently small (Hamiltonian) perturbation of $X_H$ then KAM-theory assures persistence of 3-tori and of 2-tori, parametrised by Cantor sets of (Hausdorff-)dimension 3 and 2 , respectively. Periodic orbits and equilibria persist by means of the implicit mapping theorem.

The Euler-Poinsot case of a free rigid body is not only integrable, but even *superintegrable*. From the absence of an external force we deduce an $SO(3)$-symmetry. Together with the flow of the vector field this yields the Lie algebra $\mathsf{so}(3) \oplus \mathbb{R}$ of integrals. This makes the phase space a ramified 2-torus bundle, the regular fibres now being the Eulerian 2-tori which form 4-parameter families. The flow on most of these 2-tori is quasi-periodic.

A 4-parameter family of invariant 2-tori is very degenerate. As soon as the torque excerted by an external force causes the angular momentum to move in space most of the Eulerian 2-tori are destroyed, confer the case of the heavy rigid body described above. Some of the invariant 2-tori survive the perturbation, at most they are slightly deformed. These persisting Eulerian 2-tori may help to understand the global flow of the perturbed system. Indeed, these 2-tori are the singularities of the *Cantor-fibration* of the phase space into 3-tori. The 3-tori shrink down to (persisting) normally elliptic 2-tori, and they are separated by the web of stable and unstable manifolds of (persisting) normally hyperbolic 2-tori.

Perturbing a superintegrable system allows for a greater variety of non-integrable systems that can be studied. For instance, we do not want to take the Lagrange top as "unperturbed system" since this choice would severely restrict both the rigid body and the external force field we were allowed to study. Requiring that a given system be a (small) perturbation of the free rigid body only puts a restriction on the external force which has to be small, while the rigid body may be of arbitrary shape, and also the form of the (small) external force field is not restricted.

Motivated by the 4-parameter family of invariant 2-tori in the unperturbed problem, we use the following normal form procedure. Consider a small (Hamiltonian) perturbation of the free rigid body. In the neighbourhood of *diophantine* 2-*tori* (a strong form of non-resonance) the averaged vector field is the first term of a series expansion of this 'original' perturbation — after a suitable co-ordinate transformation. The averaged Hamiltonian system is called a normal form (of order one) and has by construction a 2-torus symmetry. It is actually possible to push this 2-torus symmetry through the whole series expansion of the original system. In particular one can obtain higher order normal forms. In the examples we treat here the normal form of order one is sufficient. From the 2-torus symmetry we conclude that the normal form is an integrable system. We require this system to be nondegenerate. (If it were not we would try the normal form of order two, *etc.*) The original system differs from the normal form by the higher order terms of the series expansion. Since the original system is a small perturbation (of order $\varepsilon$ ) of the free rigid body, this difference is very small (of order $\varepsilon^2$ ). Hence we consider the original system as a perturbation of its normal form and apply KAM-theory. Note that this approach is also used in [Arnol'd;63b], [Mazzocco;97] to show the existence of invariant 3-tori in the original system.

The free rigid body with three equal principal moments of inertia is a *properly degenerate* integrable system that is degenerate even compared to superintegrable systems, all orbits are periodic. The program sketched above would only work for very special perturbations as the resulting normal form only has an $S^1$-symmetry and without further assumptions we cannot expect it to be integrable. This equally applies to perturbations of the three-dimensional Kepler problem. While a non-integrable normal form does not prevent a treatment based on Nekhoroshev's theorem, one obtains also with this approach a much better control of the dynamics close to an integrable normal form, confer [Fassò;91], [Benettin,Fassò;96], [Benettin,Fassò,Guzzo;97].

This paper is organized as follows. In the next section we give a brief summary of the basic facts about the geometry of the phase space and the form of the energy. The computations become more lucid when the rigid body is *dynamically symmetric*, and so we restrict ourselves entirely to that case. We derive the normal form and reduce to one degree of freedom. In Section 3 the resulting family of one-degree-of-freedom systems is studied in detail. From this the dynamics of the normal form in three degrees of freedom is reconstructed in Section 4. We conclude with some remarks on what this "averaged dynamics" has to do with the original perturbation problem. A more detailed treatment of this question will appear as a sequel [Hanßmann;97] to the present paper.

**Acknowledgements :** I want to thank Henk Broer for his encouragement and invaluable comments and suggestions. I also thank Richard Cushman, Sergei Dovbysh, Holger Dullin, Francesco Fassò, Jürgen Pöschel, Carles Simó and Floris Takens for stimulating discussions. The figures were drawn using the software package `DYNPAO` of Rense Posthumus, for a description see [Posthumus,Scholtmeijer;90]. The formulae have been checked with `Mathematica`, see [Wolfram;88].

## §2 Kinematics and normal form reduction

The Euler top has been thoroughly studied in the literature, confer [Abraham,Marsden;78], [Libermann,Marle;86], [Cushman,Bates;97] for the classical results and [Fassò;96] for an extensive discussion of the implications of the superintegrability of the system. In the sequel the basic facts are expressed in a form that allows us to analyse the perturbation by an external force field. In particular we emphasize the *central action* which helps to understand the geometric structure of the phase space.

A rigid body is a body in which the distances between all its component particles remain fixed under the application of a force or torque. To identify the configuration space of the rigid body with the group $SO(3)$ we choose an orthonormal basis $\{\vec{e}_x, \vec{e}_y, \vec{e}_z\}$ consisting of eigenvectors of the linear part of the force field and a body set of axes $\{\vec{e}_1, \vec{e}_2, \vec{e}_3\}$ along the principal axes of inertia. Restricting to the dynamically symmetric case $I_1 = I_2$ of two equal principal moments of inertia we may also arrange the second component of the centre of mass $\vec{s} = s_1\vec{e}_1 + s_3\vec{e}_3$ to vanish. As the potential of the affine force field reads $\alpha x + \beta y + \gamma z + ax^2 + by^2 + cz^2$ in the spatial co-ordinates $(x, y, z)$ , the potential energy of the rigid body becomes

$$\begin{aligned} V \;&=\; \alpha s_1(\vec{e}_x \,|\, \vec{e}_1) \;+\; \beta s_1(\vec{e}_y \,|\, \vec{e}_1) \;+\; \ldots \;+\; \gamma s_3(\vec{e}_z \,|\, \vec{e}_3) \\ &\quad+\; a\frac{I_3}{2}(\vec{e}_x \,|\, \vec{e}_1)^2 \;+\; b\frac{I_3}{2}(\vec{e}_y \,|\, \vec{e}_1)^2 \;+\; \ldots \;+\; c(I_1 - \frac{I_3}{2})(\vec{e}_z \,|\, \vec{e}_3)^2 \quad . \end{aligned}$$

The phase space $T^*SO(3)$ is diffeomorphic to the trivial vector bundle $SO(3) \times \mathbb{R}^3$ . However, there is no canonical choice of this diffeomorphism, or rather there are two natural choices, corresponding to measuring the angular momentum $\vec{\ell}$ in the body set of axes or in the spatial frame. This gives rise to the *body representation* $(g, \ell) \in SO(3) \times \mathbb{R}^3$ and to the *space representation* $(\mu, g) \in \mathbb{R}^3 \times SO(3)$ of a state $\alpha \in T^*_g SO(3)$ in phase space — the advantage of "reversing the order" in the latter will become clear in a moment.

To further explain the geometric structure of the phase space we use the central action $\Gamma$ . Taking out the zero-section $SO(3) \subseteq T^*SO(3)$ where the total angular momentum $|\mu| = \sqrt{\mu_1^2 + \mu_2^2 + \mu_3^2} = \sqrt{\ell_1^2 + \ell_2^2 + \ell_3^2}$ vanishes we define $\Gamma$ by means of the $2\pi$-periodic flow of the Hamiltonian vector field $X_{|\mu|}$ . As this corresponds to a pure precession about the angular momentum $\vec{\ell}$ the central action reads $\Gamma_\xi(g,\ell) = (g \cdot \exp(-\xi \frac{\ell}{\|\ell\|}), \ell)$ in the body representation and $\Gamma_\xi(\mu, g) = (\mu, \exp(-\xi \frac{\mu}{\|\mu\|}) \cdot g)$ in the space representation. The orbit space of $\Gamma$ is $\mathcal{B} = \{ (\mu, \ell) \in \mathbb{R}^3 \backslash \{0\} \times \mathbb{R}^3 \backslash \{0\} \mid \|\mu\| = \|\ell\| \}$ and dividing out the central action yields a *bifibration* $T^*SO(3)^{\backslash SO(3)} \longrightarrow \mathcal{B}$ with global action $|\mu|$ and symplectic leaves $S^2_{|\mu|} \times S^2_{|\mu|}$ , confer *Figure 2.1*. While $\mathcal{B} \longrightarrow ]0, \infty[$ is a trivial bundle, the projection $\{ \alpha \in T^*SO(3) \mid \|\alpha\| = |\mu| \} \longrightarrow S^2_{|\mu|} \times S^2_{|\mu|}$ is essentially the Hopf fibration, being *e.g.* $(\mu, g) \mapsto (\mu, g^{-1}(\mu))$ in the space representation.

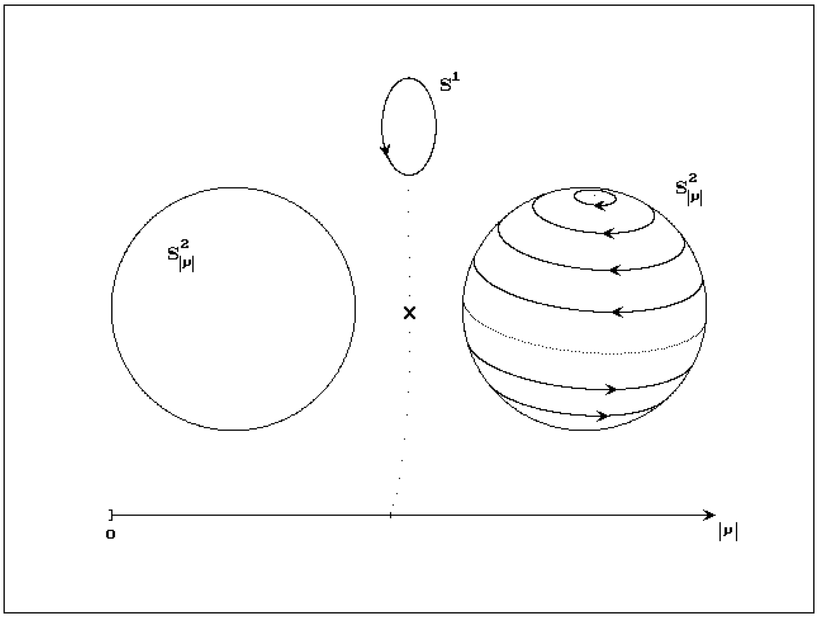


*Figure 2.1*: Schematic representation of the bundle structure of $T^*SO(3)^{\backslash SO(3)}$ .

For the Euler top the Hamilton function is the kinetic energy $T = \frac{\ell_1^2 + \ell_2^2}{2I_1} + \frac{\ell_3^2}{2I_3}$ and one can imagine the flow as depicted in the schematic representation of *Figure 2.1*. Besides the points $|\mu|$ on the interval $]0, \infty[$ also the points on the left hand sphere $S^2_{|\mu|}$ remain fixed. On the right hand sphere one has the circular flow of Euler's equations. Choosing cylindrical co-ordinates $\Im = \ell_3$ and $\rho \in S^1$ satisfying $\cos \rho = \frac{-\ell_1}{\sqrt{\ell_1^2 + \ell_2^2}}$ , $\sin \rho = \frac{\ell_2}{\sqrt{\ell_1^2 + \ell_2^2}}$ we are led to the *generalized action angle variables* $(\xi, \rho, |\mu|, \Im, \mu_1, \mu_2, \mu_3)$ of the Euler top, keeping in mind the relation $|\mu|^2 - \mu_1^2 - \mu_2^2 - \mu_3^2 = 0$ . Note that the precession angle $\xi$ can be defined only after a line through the origin, *e.g.* the $\mu_3$-axis, has been taken away out of $\mathbb{R}^3 \backslash \{0\}$ . In these variables the kinetic energy reads $\frac{|\mu|^2}{2I_1} - \frac{I_3 - I_1}{I_1 I_3} \cdot \frac{\Im^2}{2}$ , showing that the general motion of the Euler top is a *regular precession* : the body rotates about the *figure axis* $\vec{e}_3$ with frequency $-\frac{I_3 - I_1}{I_1 I_3} \Im$ , while the figure axis itself precesses about the angular momentum vector $\vec{\ell}$ with frequency $\frac{|\mu|}{I_1}$ . In the exceptional cases $\Im = 0$ and $\Im = \pm |\mu|$ the figure axis and the angular momentum coincide and one has a steady rotation about a principal axis of inertia.

We remark that the regular fibres of the ramified 2-torus bundle defined by the flow on $T^*SO(3)$ , the Eulerian 2-tori, give rise to the (dynamically defined) bifibration $T^*SO(3)\backslash\{\Im = \pm|\mu|\} \longrightarrow \{ (\mu, \Im) \in \mathbb{R}^3 \times \mathbb{R} \mid |\Im| < \|\mu\| \}$ , with global actions $|\mu|$ and $\Im$ and symplectic leaves $S^2_{|\mu|} \times \{\Im\}$ , and refer to [Fassò;96] for a further discussion. The reason why we refrein from also choosing cylindrical co-ordinates on $S^2_{|\mu|} \times \{\Im\}$ — which would lead to the Andoyer variables, confer [Andoyer;23], [Deprit;67], [Arnol'd,Kozlov,Neishtadt;85] — is that $(\mu_1, \mu_2, \mu_3)$ are globally defined on the base space and hence allow a global treatment of the one-degree-of-freedom problem we reduce to after the normalisation to which we turn now.

Let $\omega(|\mu|, \Im)$ denote the frequency vector of the parallel flow on the invariant 2-tori of the Euler top. For resonant 2-tori already a small perturbation usually leads to frequency locking. This results in some isolated periodic orbits, but the 2-torus breaks up. Therefore we single out a $(|\mu|_0, \Im_0)$ with (even) a diophantine frequency vector $\omega(|\mu|_0, \Im_0)$ and concentrate on the situation around the associated quasi-periodic tori.

We simplify and unify the notation by setting $y_1 := |\mu| - |\mu|_0$ , $y_2 := \Im - \Im_0$ , $x_1 := \xi$ , $x_2 := \rho$ , $z := (\mu_1, \mu_2, \mu_3)$ and $\varepsilon = (\alpha, \beta, \gamma, a, b, c)$ , so $x = (x_1, x_2)$ takes its values on a 2-torus $\mathsf{T}$, $y = (y_1, y_2)$ takes its values in an open part $\mathsf{Y} = \{ (y_1, y_2) \mid |\Im_0 + y_2| < |\mu|_0 + y_1 \}$ of $\mathbb{R}^2$ and $z$ takes its values in $\mathsf{P} \subseteq \mathbb{R}^3\backslash\{0\}$ . The Poisson structure on $\mathsf{T} \times \mathsf{Y} \times \mathsf{P}$ is given by *Table 2.1.*

| $\{A,B\}$ | $x_1$ | $x_2$ | $y_1$ | $y_2$ | $z_1$ | $z_2$ | $z_3$ | $B$ |
|---|---|---|---|---|---|---|---|---|
| $x_1$ | $0$ | $0$ | $1$ | $0$ | $\frac{(\|\mu\|_0+y_1)z_1}{z_1^2+z_2^2}$ | $\frac{(\|\mu\|_0+y_1)z_2}{z_1^2+z_2^2}$ | $0$ | |
| $x_2$ | $0$ | $0$ | $0$ | $1$ | $0$ | $0$ | $0$ | |
| $y_1$ | $-1$ | $0$ | $0$ | $0$ | $0$ | $0$ | $0$ | |
| $y_2$ | $0$ | $-1$ | $0$ | $0$ | $0$ | $0$ | $0$ | |
| $z_1$ | $-\frac{(\|\mu\|_0+y_1)z_1}{z_1^2+z_2^2}$ | $0$ | $0$ | $0$ | $0$ | $z_3$ | $-z_2$ | |
| $z_2$ | $-\frac{(\|\mu\|_0+y_1)z_2}{z_1^2+z_2^2}$ | $0$ | $0$ | $0$ | $-z_3$ | $0$ | $z_1$ | |
| $z_3$ | $0$ | $0$ | $0$ | $0$ | $z_2$ | $-z_1$ | $0$ | |
| $A$ | | | | | | | | |

*Table 2.1*: The Poisson bracket on $\mathsf{T} \times \mathsf{Y} \times \mathsf{P}$ . The co-ordinates on the first two factors are canonically conjugate, while the Poisson structure on the third factor reflects $\mathsf{so}(3)$ .

A short calculation shows that $(x, y, z) \mapsto (|\mu|_0 + y_1)^2 - (z \mid z)$ defines the Casimir element. With $\pi_{\mathsf{Y}}$ we denote the projection of $\mathsf{T} \times \mathsf{Y} \times \mathsf{P}$ onto the second factor. The proofs of the following results may be found in [Hanßmann;95a].

*Theorem 2.1*

*Let* $\mathsf{T}$ *be an* $n$*-torus,* $\mathsf{Y}$ *an open neighbourhood of the origin in* $\mathbb{R}^n$ *and* $\mathsf{P}$ *a Poisson space. Generate a Poisson bracket on* $\mathsf{T} \times \mathsf{Y}$ *by* $\{x_i, x_j\} = 0 = \{y_i, y_j\}$ *and* $\{x_i, y_j\} = \delta_{ij}$ *. Supply* $(\mathsf{T}\times\mathsf{Y})\times\mathsf{P}$ *with a Poisson structure that extends the brackets on* $\mathsf{T}\times\mathsf{Y}$ *and* $\mathsf{P}$ *and satisfies* $\{y_i, z_j\} = 0$ *. Let* $H(x, y, z, \varepsilon) = T(y) + V_\varepsilon(x, y, z)$ *be a perturbed Hamilton function on* $\mathsf{T} \times \mathsf{Y} \times \mathsf{P}$ *, depending on the perturbation parameter* $\varepsilon \in \mathbb{R}^m$ *. Suppose that the frequency vector* $\omega = \frac{\partial T}{\partial y}(0)$ *is diophantine. Then there is a Poisson co-ordinate transformation* $\psi$ *such that* $(H \circ \psi)(x, y, z, \varepsilon) = T(y) + \bar{V}_\varepsilon(y, z) + \mathrm{O}(\varepsilon\cdot(y + \varepsilon))$ *.*

*Corollary 2.2*

*Let* $H$ *be the Hamilton function of a rigid body, fixed at one point, with principal moments of inertia* $I_1 = I_2 \neq I_3$ *and centre of mass* $s_1\vec{e}_1 + s_3\vec{e}_3$ *, and moving in a conservative affine force field. Then the normal form of order one of* $H$ *is*

$$\begin{aligned} \bar{H}_{|\mu|,\Im}(\mu_1, \mu_2, \mu_3) \;=\; & \frac{|\mu|^2}{2I_1} - \frac{I_3 - I_1}{I_1 I_3}\frac{\Im^2}{2} + \frac{a+b+c}{2}(I_1 + (I_3 - I_1)\frac{\Im^2}{|\mu|^2}) \\ & + s_3\frac{\Im}{|\mu|}(\alpha\frac{\mu_1}{|\mu|} + \beta\frac{\mu_2}{|\mu|} + \gamma\frac{\mu_3}{|\mu|}) - \frac{I_3 - I_1}{2}\frac{3\Im^2 - |\mu|^2}{|\mu|^2}(a\frac{\mu_1^2}{|\mu|^2} + b\frac{\mu_2^2}{|\mu|^2} + c\frac{\mu_3^2}{|\mu|^2}) \quad . \end{aligned} \tag{1}$$

Note that the averaged Hamilton function $\bar{H}$ is defined on the whole phase space $T^*SO(3)^{\backslash SO(3)}$ , while the transformations $\psi$ are only locally defined. We are concerned with motions that stay *à priori* in a specified chart of the generalized action angle variables. In case one is interested in the fate of motions on those $X_{\bar{H}}$-invariant tori that get destroyed, for instance to get Nekhoroshev estimates on the time variation of $|\mu|$ and $\Im$ , such “local” considerations are no longer sufficient. A global formulation of Hamiltonian perturbation theory is obtained in [Fassò;91,94,95]. The local expressions $\psi$ are shown to represent a unique co-ordinate transformation that is globally defined on the symplectic leaves $S^2_{|\mu|} \times \{\Im\}$ , with $(|\mu|, \Im)$ varying in some appropriate domain.

The normal form $\bar{H}$ is invariant under the central action $\Gamma$ and under rotations about the figure axis. These two $S^1$-actions commute and define a 2-torus action. The corresponding *momentum mapping* is

$$(|\mu|, \Im) : \;\; T^*SO(3) \;\longrightarrow\; \mathbb{R}^2 \quad .$$

The level sets of the momentum mapping are invariant manifolds of the Hamiltonian vector field $X_{\bar{H}}$ . These level sets are also invariant under the 2-torus action. In the schematic representation of *Figure 2.1* the level sets correspond to fixed radius $|\mu|$ of the two spheres and fixed height $\Im$ on the right hand sphere $S^2_{|\mu|}$ . The 2-torus action rotates along the $S^1$-fibres and along circles of height $\Im$ on the right hand sphere. Dividing out this action leads to the reduced phase space $S^2_{|\mu|} \times \{\Im\}$ , on which the reduced Hamilton function $\bar{H}_{|\mu|,\Im}$ defines a one-degree-of-freedom problem. This suggests the following three-step program.

First the one-degree-of-freedom problem has to be understood. Here one has to investigate a Hamilton function $\bar{H}_{|\mu|,\Im}$ on $S^2_{|\mu|} \times \{\Im\}$ . At this point we see whether the study of the normal form of order one can lead to information on the original system. We require the one-degree-of-freedom problem to be *structurally stable* as a family, parametrised by the two actions. We use (parameter-dependent) singularity theory to identify the equilibria. These equilibria correspond to invariant 2-tori for the averaged Hamilton function $\bar{H}$ on $T^*SO(3)^{\setminus SO(3)}$ .

In the second step one has to reconstruct the dynamics of $X_{\bar{H}}$ on $T^*SO(3)^{\setminus SO(3)}$ from the one-degree-of-freedom problems. Each point of $S^2_{|\mu|} \times \{\Im\}$ gets a 2-torus attached and $T^*SO(3)^{\setminus SO(3)}$ is the union of these 4-dimensional invariant manifolds. The dynamics on $S^2_{|\mu|} \times \{\Im\}$ lifts to $T^*SO(3)^{\setminus SO(3)}$ . In particular we reconstruct invariant 2-tori from the equilibria on $S^2_{|\mu|} \times \{\Im\}$ . The *energy-momentum mapping*

$$(\bar{H}, |\mu|, \Im) : \quad T^*SO(3)^{\setminus SO(3)} \quad \longrightarrow \quad \mathbb{R}^3$$

makes the phase space a ramified torus bundle, the regular fibres being invariant 3-tori. The invariant 2-tori are contained in singular fibres of this bundle, in the normally hyperbolic case the fibre includes the stable and unstable manifolds. They appear for critical values of the energy-momentum mapping.

The third and final step has to show what the "averaged dynamics" to $X_{\bar{H}}$ has to do with the rigid body motion as described by $X_H$ . The step from $\bar{H}$ to $H$ is actually a perturbation in itself. If the perturbation $V$ of $T$ is of order $\varepsilon$ , we want $\bar{H} = T + \bar{V}$ to be a perturbation of $H = T + V$ of order $\varepsilon^2$ . From ordinary KAM-theory, see [Arnol'd;63b], [Pöschel;82] and [Mazzocco;97], we know that most of the invariant 3-tori survive the perturbation. These 3-tori survive as a 3-dimensional *Cantor family*. Using a centre manifold one can similarly show that normally hyperbolic invariant 2-tori survive the perturbation as a 2-dimensional Cantor family, see also [Graff;74]. For normally elliptic invariant 2-tori we use the theory of [Moser;67] and [Broer,Huitema,Takens;90]. It turns out that also the normally elliptic invariant 2-tori survive the perturbation as a 2-dimensional Cantor family. However, the parametrising Cantor sets for normally hyperbolic and for normally elliptic 2-tori have different structures.

## §3 The one-degree-of-freedom system

The first step of our program is to study the parametrised Hamilton function $\bar{H}_{|\mu|,\Im}$ of Corollary 2.2 on $S^2_{|\mu|} \times \{\Im\}$ . We consider the external parameters $\alpha, \beta, \gamma, a, b, c$ as fixed constants. The internal or *distinguished parameters* $|\mu|$ and $\Im$ on the other hand are allowed to vary. We want to show that this family of one-degree-of-freedom problems is structurally stable in the subclass of (families of) Hamiltonian systems on $S^2_{|\mu|} \times \{\Im\}$ .

Let us start with a rough description of the expected phase portraits. For an open and dense part of the parameter plane the corresponding system $X_{\bar{H}_{|\mu|,\Im}}$ itself is structurally stable, here $\bar{H}_{|\mu|,\Im}$ is a Morse function. The flow on $S^2_{|\mu|} \times \{\Im\}$ mostly consists of periodic orbits and can be characterized by the distribution of its equilibria. The occurring cases have, respectively, four centres and two saddles, or three centres and one saddle, or two centres. To understand the whole family $\bar{H}_{|\mu|,\Im}$ we also study the bifurcations between these structurally stable systems. To pass from one of the above cases to another a centre and a saddle have to meet in a *centre-saddle bifurcation* and vanish. We also encounter a *connection bifurcation* where the two saddles have the same energy.

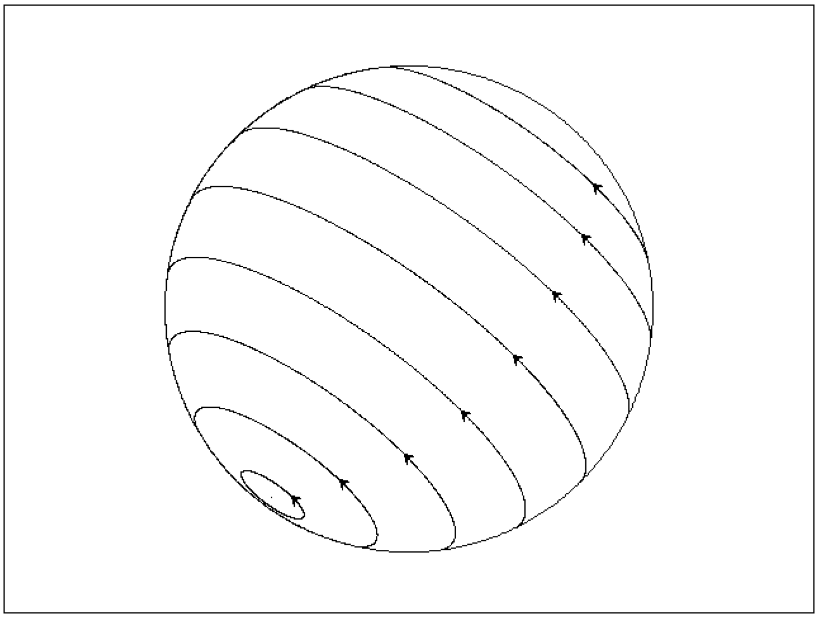

*Figure 3.1*: The flow on $S^2_{|\mu|}$ to the reduced Hamilton function $\bar{H}_{|\mu|,\Im}$ for $3\Im^2 \approx |\mu|^2$ .

To be more explicit, the orbits of the Hamiltonian vector field $X_{\bar{H}_{|\mu|,\Im}}$ are the intersections of the quadrics $\{ \bar{H}_{|\mu|,\Im}(\mu_1, \mu_2, \mu_3) = h \} \subseteq \mathbb{R}^3$ with $S^2_{|\mu|}$ (from now on we drop the factor $\{\Im\}$ in $S^2_{|\mu|} \times \{\Im\}$ ). Let us see how this information can be used to obtain the phase portraits.

If $3\Im^2 = |\mu|^2$ the intersections of the level sets $\{\bar{H}_{|\mu|,\Im} = h\}$ with $S^2_{|\mu|}$ are "lines of equal height" — with "height" increasing in direction $\begin{pmatrix} \alpha \\ \beta \\ \gamma \end{pmatrix}$ ; see *Figure 3.1*. In this case the quadratic part of the potential energy has no influence. For $3\Im^2 \neq |\mu|^2$ the level sets of $\bar{H}_{|\mu|,\Im}$ are triaxial ellipsoids with centre

$$\frac{s_3 \, \Im \, |\mu|}{(I_3 - I_1)(3\Im^2 - |\mu|^2)} \begin{pmatrix} \alpha/a \\ \beta/b \\ \gamma/c \end{pmatrix} .$$

When $(|\mu|, \Im) \longrightarrow \{3\Im^2 = |\mu|^2\}$ this centre tends to infinity. Let us consider values $(|\mu|, \Im)$ near $\{3\Im^2 = |\mu|^2\}$ . When it comes to an intersection of the ellipsoid $\{\bar{H}_{|\mu|,\Im} = h\}$ with the sphere $S^2_{|\mu|}$ , the curvature of the ellipsoid is so small that locally, *i.e.* on the sphere, it resembles a plane. Qualitatively the flow remains as depicted in *Figure 3.1*. We get 2 centres, surrounded by periodic orbits.

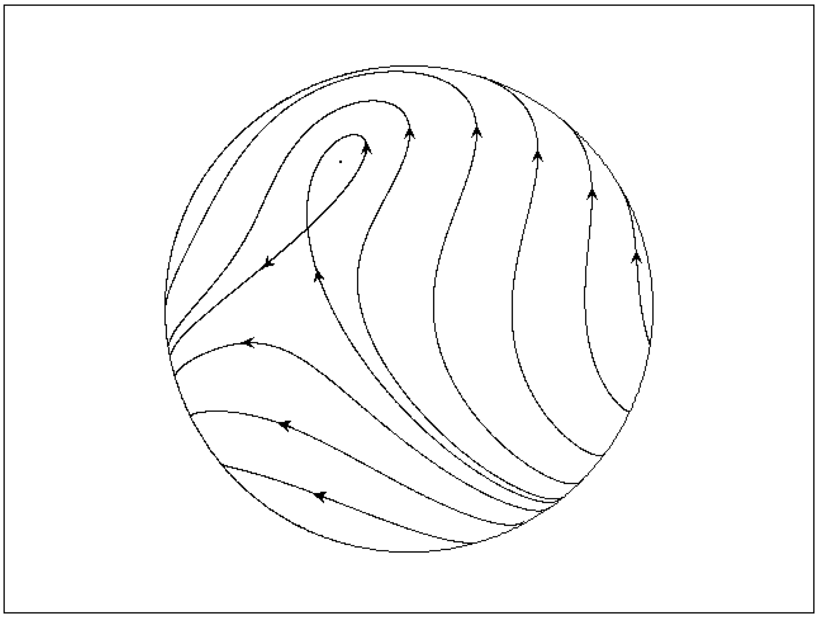

*Figure 3.2*: A possible flow on $S^2_{|\mu|}$ to the reduced Hamilton function $\bar{H}_{|\mu|,\Im}$ for $3\Im^2 \neq |\mu|^2$ .

Now let the centre of the ellipsoid be closer to $S^2_{|\mu|}$ . We start with a big ellipsoid $\{\bar{H}_{|\mu|,\Im} = h\}$ that completely contains the sphere $S^2_{|\mu|}$ . When the ellipsoid gets smaller there is an energy $h$ for which it touches $S^2_{|\mu|}$ in one point. After this we get periodic orbits around this centre. There is another energy $h$ for which, next to such a circle of intersection, the ellipsoid touches $S^2_{|\mu|}$ in an isolated point. When the ellipsoid shrinks further the two periodic orbits around the two equilibria merge into a "figure 8". Still decreasing in size, the ellipsoid intersects $S^2_{|\mu|}$ in one periodic orbit which shrinks down to another centre. This equilibrium corresponds to the point in which $S^2_{|\mu|}$ touches the ellipsoid before lying completely outside $\{\bar{H}_{|\mu|,\Im} = h\}$ . Confer *Figure 3.2.* The "figure 8" consists of a saddle together with two homoclinic orbits that form its stable (and unstable) manifolds. When the centre of the ellipsoid lies inside $S^2_{|\mu|}$ one can get another "figure 8". In this case the flow to $\bar{H}_{|\mu|,\Im}$ on $S^2_{|\mu|}$ has five families of periodic orbits. Four of these families shrink to centres. The five families are separated by the (un)stable manifolds of two saddles.

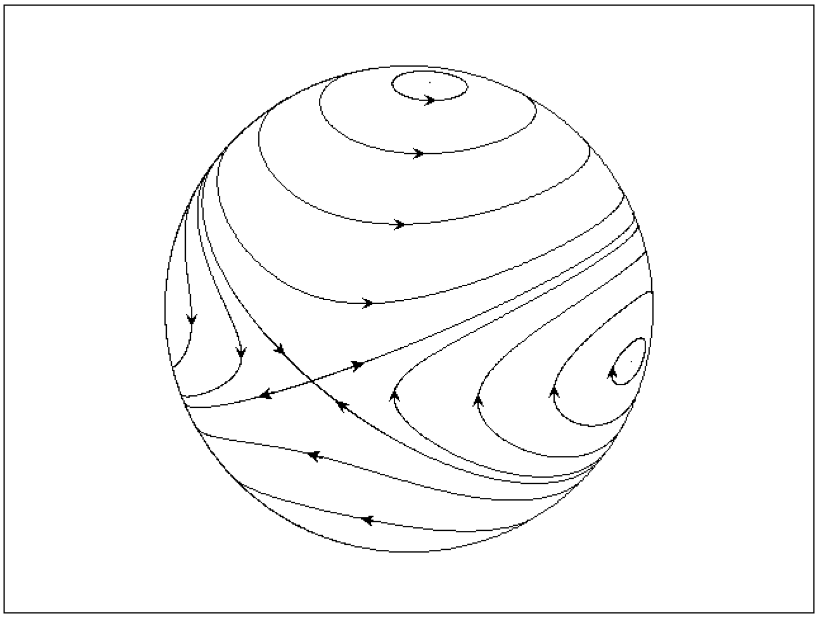

*Figure 3.3*: The flow on $S^2_{|\mu|}$ to the reduced Hamilton function $\bar{H}_{|\mu|,0}$ .

If $\Im = 0$ the centre of the ellipsoid coincides with the origin. The fifth family of periodic orbits disappears and the two saddles become connected by heteroclinic orbits, see *Figure 3.3.* In this case the linear part of the potential energy has no influence. There are two other nongeneric cases, connected with appearances of a "figure 8". Imagine the smaller of the loops of the "figure 8" shrinking down to a point. This point corresponds to a *parabolic* equilibrium, with linearisation $\left(\begin{smallmatrix} 0 & 1 \\ 0 & 0 \end{smallmatrix}\right)$ . The "remaining" loop of the "figure 8" is the homoclinic orbit to this equilibrium. Together with the parabolic equilibrium the homoclinic orbit forms a topological circle which has a cusp at the equilibrium. From both sides this circle is approximated by periodic orbits, the period of which tends to infinity. Locally this situation is described by the centre-saddle bifurcation, confer *Figure 3.4* ; the Hamilton function undergoes a fold catastrophe, see also [Broer,Chow,Kim,Vegter;93]. Note that the nongeneric Hamiltonian vector fields $X_{\bar{H}_{|\mu|,\Im}}$ on $S^2_{|\mu|}$ correspond to isolated values of $\frac{\Im}{|\mu|}$ , the phenomena have co-dimension one. Here 'nongeneric' is understood within the space of all Hamiltonian vector fields.

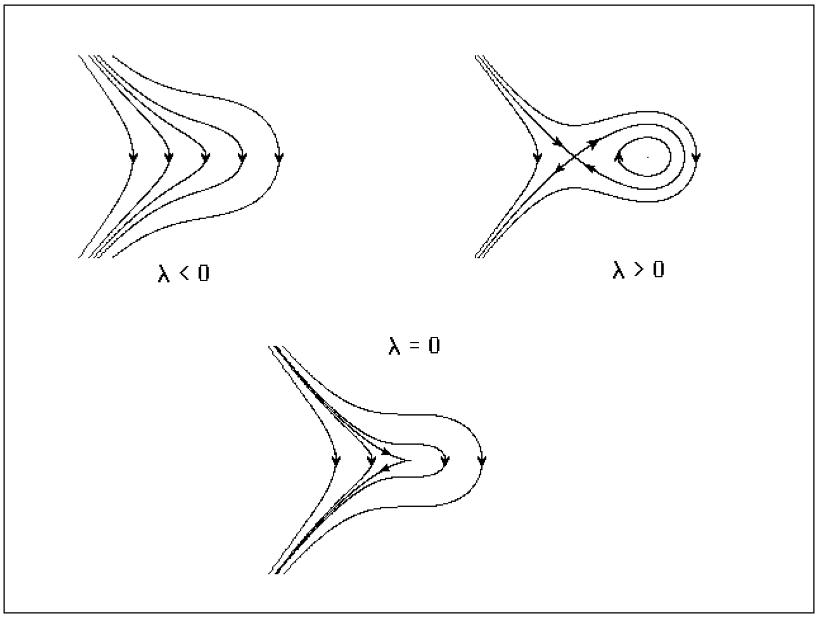


*Figure 3.4*: The Hamiltonian centre-saddle bifurcation.

To prove that the reduced normal form $\bar{H}_{|\mu|,\Im}$ indeed defines a structurally stable family we may neglect the first three terms of (1). The two remaining terms are invariant under the transformation $\mu \mapsto \frac{\mu}{|\mu|}$ (which turns $\Im$ into $\frac{\Im}{|\mu|}$ ). Multiplying these terms by $\frac{1}{I_3-I_1} \cdot \frac{|\mu|^2}{|\mu|^2-3\Im^2}$ we are led to

$$\mathcal{H}_{\mathcal{I}}(x,y,z) \;=\; \mathcal{I}\,(\alpha x+\beta y+\gamma z) \;+\; \frac{1}{2}(ax^2+by^2+cz^2) \tag{2}$$

with $x=\frac{\mu_1}{|\mu|}$ , $y=\frac{\mu_2}{|\mu|}$ , $z=\frac{\mu_3}{|\mu|}$ and $\mathcal{I}=\frac{s_3}{I_3-I_1}\cdot\frac{\Im\,|\mu|}{|\mu|^2-3\Im^2}$ . This shows already why we only encountered bifurcations of co-dimension one : the two-parameter family $\bar{H}_{|\mu|,\Im}$ is induced by the one-parameter family $\mathcal{H}_{\mathcal{I}}$ . The reason behind this is that $|\mu|$ and $\Im$ enter only as quotient $\frac{\Im}{|\mu|}$ in $V_{\alpha,\beta,\gamma,a,b,c}$ . Indeed, the potential energy depends only on the configuration $g\in SO(3)$ of the system.

*Theorem 3.1*

*Let $(\alpha,\beta,\gamma,a,b,c)$ be in $\mathbb{R}^6$ with $\alpha,\beta,\gamma>0$ and $a<b<c$ . Then the one-parameter family $\mathcal{H}_{\mathcal{I}}$ of Hamiltonian systems defined by (2) is structurally stable on $S^2$ .*

Proof :

Define the polynomials $f_1, f_2, f_3, f_4, f_5, f_6 \in \mathbb{R}[\lambda]$ by

$$
\begin{aligned}
f_i(\lambda) &:= \alpha^2(\lambda-b)^i(\lambda-c)^i+\beta^2(\lambda-a)^i(\lambda-c)^i+\gamma^2(\lambda-a)^i(\lambda-b)^i \quad , {\scriptstyle i=1,2,3} \\
f_4(\lambda) &:= \beta^2(\lambda-c)^2+\gamma^2(\lambda-b)^2 \\
f_5(\lambda) &:= (\lambda-a)(\lambda-b)(\lambda-c) \\
f_6(\lambda) &:= \alpha^2(\lambda-\tfrac{a}{2})(\lambda-b)^2(\lambda-c)^2 \\
&\quad +\beta^2(\lambda-a)^2(\lambda-\tfrac{b}{2})(\lambda-c)^2+\gamma^2(\lambda-a)^2(\lambda-b)^2(\lambda-\tfrac{c}{2}) \quad .
\end{aligned}
$$

To show structural stability we study the behaviour of the equilibria of $X_{\mathcal{H}_\mathcal{I}}$ on $S^2$ . We have to solve the equation

$$
\begin{pmatrix} \frac{\partial \mathcal{H}_\mathcal{I}}{\partial x} \\ \frac{\partial \mathcal{H}_\mathcal{I}}{\partial y} \\ \frac{\partial \mathcal{H}_\mathcal{I}}{\partial z} \end{pmatrix} = \lambda \cdot \begin{pmatrix} x \\ y \\ z \end{pmatrix}
$$

under the condition $x^2+y^2+z^2=1$ . Solving the equation for $x, y$ and $z$ the condition reads $f_2(\lambda)\,\mathcal{I}^2 = (f_5(\lambda))^2$ . The solutions of this sixth degree polynomial in $\lambda$ yield the equilibria, for fixed $\mathcal{I}$ there are between two and six of them. We use the Lagrange multiplier $\lambda$ as a parameter for

$$
x^\epsilon_\lambda = \frac{\mathcal{I}^\epsilon(\lambda)\,\alpha}{\lambda-a} \quad , \quad y^\epsilon_\lambda = \frac{\mathcal{I}^\epsilon(\lambda)\,\beta}{\lambda-b} \quad , \quad z^\epsilon_\lambda = \frac{\mathcal{I}^\epsilon(\lambda)\,\gamma}{\lambda-c}
$$

with $\mathcal{I}^\epsilon(\lambda) = \dfrac{\epsilon\, f_5(\lambda)}{\sqrt{f_2(\lambda)}}$ and $\epsilon = \pm 1$ . These two families of equilibria have the (common) energy

$$
\mathcal{H}_{\mathcal{I}^\epsilon(\lambda)}(x^\epsilon_\lambda, y^\epsilon_\lambda, z^\epsilon_\lambda) = \frac{f_6(\lambda)}{f_2(\lambda)} =: h(\lambda) \quad .
$$

The two curves $(\mathcal{I}^\epsilon(\lambda), h(\lambda))$ intersect in the points $(0,\frac{a}{2}), (0,\frac{b}{2})$ and $(0,\frac{c}{2})$ , corresponding to the equilibria $(\epsilon,0,0), (0,-\epsilon,0)$ and $(0,0,\epsilon)$ . Therefore $\mathcal{I}^\epsilon(\lambda)$ has relative maxima and relative minima. A direct computation shows

$$
\frac{\mathrm{d}}{\mathrm{d}\lambda}(\mathcal{I}^\epsilon(\lambda), h(\lambda)) = \frac{f_3(\lambda)}{(\sqrt{f_2(\lambda)})^3}\,(1, \frac{f_1(\lambda)}{\sqrt{f_2(\lambda)}}) \quad ,
$$

so the relative extrema correspond to cusp points, confer *Figure 3.5.* To prove that $f_3$ has indeed exactly two real roots $\lambda_-$ and $\lambda_+$ we divide by $f_5^3$ , thus introducing three poles at $a, b$ and $c$ . As

$$
\frac{\mathrm{d}}{\mathrm{d}\lambda}\frac{f_3(\lambda)}{(f_5(\lambda))^3} = -\frac{\alpha^2}{(\lambda-a)^4} - \frac{\beta^2}{(\lambda-b)^4} - \frac{\gamma^2}{(\lambda-c)^4} < 0 \quad ,
$$

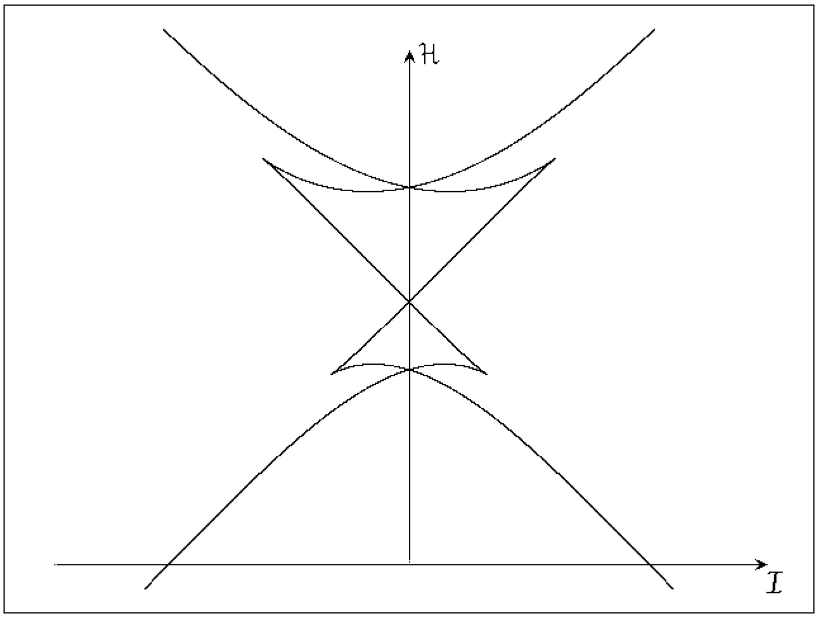


*Figure 3.5*: The two curves $(\mathcal{I}^{\pm}(\lambda), h(\lambda))$ .

the quotient is strictly decreasing, yielding unique roots $\lambda_- \in \,]a,b[$ and $\lambda_+ \in \,]b,c[$ . These satisfy $f_3'(\lambda_-) < 0$ and $f_3'(\lambda_+) > 0$ , and on $]-\infty,a] \cup [c,\infty[$ we have $f_3 \geq (c-a)^3 \cdot \min(\alpha^2(b-a)^3, \gamma^2(c-b)^3) > 0$ .
In the neighbourhood of the equilibria we choose local co-ordinates $Q$ and $P$ on $S^2$ according to

$$\begin{pmatrix} x \\ y \\ z \end{pmatrix} \stackrel{!}{=} \sqrt{1-Q^2-P^2}\begin{pmatrix} x_\lambda^\epsilon \\ y_\lambda^\epsilon \\ z_\lambda^\epsilon \end{pmatrix} + \frac{Q}{\sqrt{(y_\lambda^\epsilon)^2+(z_\lambda^\epsilon)^2}}\begin{pmatrix} 0 \\ -z_\lambda^\epsilon \\ y_\lambda^\epsilon \end{pmatrix}$$
$$+ \frac{P}{\sqrt{(y_\lambda^\epsilon)^2+(z_\lambda^\epsilon)^2}}\begin{pmatrix} (y_\lambda^\epsilon)^2+(z_\lambda^\epsilon)^2 \\ -x_\lambda^\epsilon\, y_\lambda^\epsilon \\ -x_\lambda^\epsilon\, z_\lambda^\epsilon \end{pmatrix} .$$

Geometrically this corresponds to a projection along the equilibrium vector. In particular $Q$ and $P$ are not symplectic co-ordinates, having Poisson bracket $\{Q,P\} = \frac{1}{|\mu|}\sqrt{1-Q^2-P^2}$ . We are interested in the equilibria corresponding to the cusp points and may assume $\lambda > a$ . Then the equations for the new co-ordinates become

$$\begin{aligned}
x(Q,P) &= \tfrac{\epsilon\alpha(\lambda-b)(\lambda-c)}{\sqrt{f_2(\lambda)}}\sqrt{1-Q^2-P^2} + \tfrac{(\lambda-a)\sqrt{f_4(\lambda)}}{\sqrt{f_2(\lambda)}}P \\
y(Q,P) &= \tfrac{\epsilon\beta(\lambda-a)(\lambda-c)}{\sqrt{f_2(\lambda)}}\sqrt{1-Q^2-P^2} - \tfrac{\epsilon\gamma(\lambda-b)}{\sqrt{f_4(\lambda)}}Q - \tfrac{\alpha\beta(\lambda-b)(\lambda-c)^2}{\sqrt{f_4(\lambda)}\sqrt{f_2(\lambda)}}P \\
z(Q,P) &= \tfrac{\epsilon\gamma(\lambda-a)(\lambda-b)}{\sqrt{f_2(\lambda)}}\sqrt{1-Q^2-P^2} + \tfrac{\epsilon\beta(\lambda-c)}{\sqrt{f_4(\lambda)}}Q - \tfrac{\alpha\gamma(\lambda-b)^2(\lambda-c)}{\sqrt{f_4(\lambda)}\sqrt{f_2(\lambda)}}P \quad .
\end{aligned}$$

Writing $\mathcal{I} = \mathcal{I}^\epsilon(\lambda) + \nu$ the 3-jet of $\mathcal{H}_\mathcal{I}$ in $Q$ and $P$ reads

$$\begin{aligned} \mathcal{H}^{\text{3-jet}}_{\lambda,\nu,\epsilon}(Q,P) \;&=\; h(\lambda) \;+\; \nu\frac{\epsilon\, f_1(\lambda)}{\sqrt{f_2(\lambda)}} \;+\; \left(\nu \;+\; \frac{\epsilon\, f_5(\lambda)}{\sqrt{f_2(\lambda)}}\frac{Q^2+P^2}{2}\right)\times \\ &\times\left(\frac{\epsilon(b-c)\beta\gamma}{\sqrt{f_4(\lambda)}}Q + \frac{(b-a)\alpha\beta^2(\lambda-c)^2 \;+\; (c-a)\alpha\gamma^2(\lambda-b)^2}{\sqrt{f_2(\lambda)}\,\sqrt{f_4(\lambda)}}P\right) \\ &+\; g_1(\lambda)P^2 \;+\; g_2(\lambda)Q^2 \;+\; \epsilon g_3(\lambda)PQ \;-\; \nu\frac{\epsilon\, f_1(\lambda)}{2\sqrt{f_2(\lambda)}}(Q^2+P^2) \quad . \end{aligned}$$

Here and in the sequel we use the algebraic functions $g_1, g_2, g_3, g_4, g_5, g_6^\tau, g_7, g_8^\tau : \mathbb{R} \longrightarrow \mathbb{R}$, $\tau = \pm 1$ , defined by

$$\begin{aligned} g_1(\lambda) \;&:=\; \tfrac{a(\lambda-a)^2 f_4(\lambda)}{2\, f_2(\lambda)} + \tfrac{b\,\alpha^2\beta^2(\lambda-b)^2(\lambda-c)^4 + c\,\alpha^2\gamma^2(\lambda-b)^4(\lambda-c)^2}{2\, f_2(\lambda)\, f_4(\lambda)} - \tfrac{\lambda}{2} \\ g_2(\lambda) \;&:=\; \tfrac{c\,\beta^2(\lambda-c)^2 + b\,\gamma^2(\lambda-b)^2}{2\, f_4(\lambda)} - \tfrac{\lambda}{2} \\ g_3(\lambda) \;&:=\; \tfrac{(b-c)\alpha\beta\gamma(\lambda-b)^2(\lambda-c)^2}{f_4(\lambda)\sqrt{f_2(\lambda)}} \\ g_4(\lambda) \;&:=\; g_1(\lambda) \;-\; g_2(\lambda) \\ g_5(\lambda) \;&:=\; \sqrt{(g_3(\lambda))^2 + (g_4(\lambda))^2} \\ g_6^\tau(\lambda) \;&:=\; \sqrt{2(g_5(\lambda))^2 - 2\tau g_4(\lambda) g_5(\lambda)} \\ g_7(\lambda) \;&:=\; \tfrac{(b+c-2a)\alpha^2(\lambda-b)^2(\lambda-c)^2 + (c-a)\beta^2(\lambda-a)^2(\lambda-c)^2 + (b-a)\gamma^2(\lambda-a)^2(\lambda-b)^2}{2\, f_2(\lambda)} \\ g_8^\tau(\lambda) \;&:=\; \tfrac{(b-c)\beta\gamma g_3(\lambda)}{g_6^\tau(\lambda)\sqrt{f_4(\lambda)}} + \tfrac{[(b-a)\alpha\beta^2(\lambda-c)^2 + (c-a)\alpha\gamma^2(\lambda-b)^2](g_4(\lambda) - \tau g_5(\lambda))}{g_6^\tau(\lambda)\sqrt{f_2(\lambda)}\sqrt{f_4(\lambda)}} \quad . \end{aligned}$$

A direct computation shows

$$\det D^2\mathcal{H}_{\lambda,0,\epsilon}(0,0) \;=\; \frac{f_3(\lambda)}{f_2(\lambda)} \qquad \text{and} \qquad \operatorname{trace} D^2\mathcal{H}_{\lambda,0,\epsilon}(0,0) \;=\; -\frac{1}{3}\frac{f_3'(\lambda)}{f_2(\lambda)} \quad ,$$

so the cusp points given by $\lambda_+$ and $\lambda_-$ correspond to parabolic equilibria on $S^2$ . Near $\lambda_\tau$ , $\tau = \pm 1$ , we use the rotation

$$\begin{pmatrix} P \\ Q \end{pmatrix} \;:=\; \frac{1}{g_6^\tau(\lambda)} \begin{pmatrix} g_4(\lambda) - \tau g_5(\lambda) & -\epsilon\, g_3(\lambda) \\ \epsilon\, g_3(\lambda) & g_4(\lambda) - \tau g_5(\lambda) \end{pmatrix} \begin{pmatrix} p \\ q \end{pmatrix}$$

as principal axis transformation. The Poisson bracket remains $\{q,p\} = \frac{1}{|\mu|}\sqrt{1-q^2-p^2}$ , and the 3-jet $\mathcal{H}^{\text{3-jet}}_{\lambda,\nu,\epsilon}$ becomes at $\lambda = \lambda_\tau$

$$\mathcal{H}^{\text{3-jet}}_{\lambda_\tau,\nu,\epsilon}(q,p) \;=\; h(\lambda_\tau) \;+\; \nu\frac{\epsilon\, f_1(\lambda_\tau)}{\sqrt{f_2(\lambda_\tau)}} \;+\; g_8^\tau(\lambda_\tau)\left(\nu \;+\; \frac{\epsilon\, f_5(\lambda)}{\sqrt{f_2(\lambda)}}\frac{q^2+p^2}{2}\right) p$$

$$
\begin{aligned}
&+\ \nu\,\epsilon\,(c-b)\beta\gamma\frac{\tau g_5(\lambda_\tau)+g_7(\lambda_\tau)}{g_6^\tau(\lambda_\tau)\sqrt{f_4(\lambda_\tau)}}\,q \\
&-\ \frac{1}{3}\frac{f_3'(\lambda_\tau)}{f_2(\lambda_\tau)}p^2\ -\ \nu\frac{\epsilon\, f_1(\lambda_\tau)}{\sqrt{f_2(\lambda_\tau)}}\,(q^2+p^2) \\
&+\ \frac{f_5(\lambda_\tau)}{\sqrt{f_2(\lambda_\tau)}}(c-b)\beta\gamma\frac{\tau g_5(\lambda_\tau)+g_7(\lambda_\tau)}{g_6^\tau(\lambda_\tau)\sqrt{f_4(\lambda_\tau)}}\,q\,\frac{q^2+p^2}{2} \qquad .
\end{aligned}
$$

To show that a centre-saddle bifurcation takes place we have to check that the coefficients of $p^2, q^3$ and $\nu q$ are nonzero. The coefficient of $p^2$ is $\operatorname{trace} D^2\mathcal{H}_{\lambda,0,\epsilon}(0,0)$ and has sign $-\tau$ . For the other two coefficients we need to know that $g_5 < g_7$ , which follows from $(g_7(\lambda))^2 - (g_5(\lambda))^2 = \frac{(b-a)(c-a)\alpha^2(\lambda-b)^2(\lambda-c)^2}{f_2(\lambda)}$ . Hence, the coefficient of $q^3$ has sign $-\tau$ , while the sign of the coefficient of $\nu q$ is $\epsilon$ .
In particular the arcs extending between the cusp points correspond to saddles (this also follows from the topological fact that the number of saddles on the sphere $S^2$ equals the number of centres minus 2 ). If we parametrise the saddles by $\mathcal{I}$ (with $(x_0^+, y_0^+, z_0^+) = (0,-1,0)$ and $(x_0^-, y_0^-, z_0^-) = (0,+1,0)$ ) we obtain

$$
\frac{\mathrm{d}}{\mathrm{d}\mathcal{I}}\Big(\mathcal{H}_\mathcal{I}(x_\mathcal{I}^+, y_\mathcal{I}^+, z_\mathcal{I}^+) - \mathcal{H}_\mathcal{I}(x_\mathcal{I}^-, y_\mathcal{I}^-, z_\mathcal{I}^-)\Big)_{|\mathcal{I}=0} \quad = \quad -2\,\beta
$$

which shows the robustness of the heteroclinic connection ; **q.e.d.**

Note that we do not distinguish between $|\mathcal{I}^\epsilon(\lambda_-)| < |\mathcal{I}^\epsilon(\lambda_+)|$ and $|\mathcal{I}^\epsilon(\lambda_-)| > |\mathcal{I}^\epsilon(\lambda_+)|$ . In case $\mathcal{I}^\pm(\lambda_-) = \mathcal{I}^\mp(\lambda_+)$ two centre-saddle bifurcations occur for the same value of $\mathcal{I}$ . Since these do not "interact" we do not have to exclude this case (as long as we keep in mind that the occurrence of two centre-saddle bifurcations at the same $\mathcal{I}$-level is not robust). The relative position of the two roots of $f_1$ with respect to $\lambda_+$ and $\lambda_-$ determines in which quadrants the tangents at the cusp points lie. One of the four generic possiblities is depicted in *Figure 3.5.* For $f_1(\lambda_\tau) = 0$ the corresponding cusp point has a horizontal tangent, in such a case the "frequency" $\frac{\partial\mathcal{H}_\mathcal{I}}{\partial\mathcal{I}}$ vanishes and the energy cannot be used as bifurcation parameter.

Let $K = T + U$ be the "constant truncation" of the Hamilton function $H = T + V$ describing a rigid body in a general conservative force field, $U$ being the potential energy given by the constant part of the force field (*i.e.* $U$ is the linear part of $V$ ). Suppose the higher order terms $V - U$ are sufficiently "small", even with respect to the "small" perturbation $U$ of $T$ . What is the relation between $\bar{K}_{|\mu|,\Im}$ and $\bar{H}_{|\mu|,\Im}$ ? The one-degree-of-freedom problem defined by $\bar{K}_{|\mu|,\Im}$ has an $S^1$-symmetry about the direction of the constant force, the affine force field being the lowest possible truncation with broken $S^1$-symmetry. However, it also does lead to structurally stable one-degree-of-freedom systems, confer *Figure 3.1.* The only exception occurs at $\Im = 0$ where $X_{\bar{K}_{|\mu|,\Im}}$ vanishes. This shows that for general $V$ the families of one-degree-of-freedom systems defined by normal forms of $K$ and $H$ cannot be equivalent. If we want to obtain information on $X_{\bar{H}}$ from $\bar{K}$ , we have to exclude a strip around $\Im = 0$ from $T^*SO(3)$ . The width of this strip can be estimated from the higher order terms $\bar{V} - \bar{U}$ , for instance the quasi-periodic centre-saddle bifurcations of the "affine truncation" take place within this strip.

Quadratic Hamiltonians on the sphere often appear after a reduction to one degree of freedom, confer the references in [Lanchares,Elipe;95a,b], [Lanchares,Iñarrea,Salas,Sierra,Elipe;95]. Studied in its own right, one can reduce the general family $\frac{a}{2}x^2 + \frac{b}{2}y^2 + \frac{c}{2}z^2 + \alpha x + \beta y + \gamma z$ to the four-parameter family

$$\mathcal{H}_{P,Q,R,S}(x,y,z) \;=\; \frac{1}{2}x^2 + \frac{P}{2}y^2 + Qx + Ry + Sz \tag{3}$$

by substracting the Casimir $\frac{c}{2}(x^2 + y^2 + z^2)$ and rescaling time. The two- and three-parameter subfamilies of (3) with $P \cdot Q \cdot R \cdot S = 0$ have been studied in [Lanchares,Elipe;95a,b] and [Lanchares,Iñarrea,Salas,Sierra,Elipe;95], respectively. In combination with Theorem 3.1 this allows to obtain the complete bifurcation diagram of the four-parameter family (3), see [Elipe,Hanßmann;97].

## §4 Reconstruction of the averaged flow

In the previous section we gave a detailed description of the one-degree-of-freedom systems $X_{\bar{H}_{|\mu|,\Im}}$ on $S^2_{|\mu|} \times \{\Im\}$ . The second step of our program consists in reconstructing the dynamics of $X_{\bar{H}}$ on $T^*SO(3)\backslash SO(3)$ from these one-degree-of-freedom systems. We have to solve two problems. On the one hand, we have to reconstruct the dynamics on the 4-dimensional invariant manifolds of constant $|\mu|$ and $\Im$ . We obtain a ramified torus bundle, the regular fibres of which are invariant 3-tori. On the other hand, we want to understand how the global flow on $T^*SO(3)\backslash SO(3)$ is organized. We have to answer questions like : what is the topology of the bundle of invariant 3-tori ? how are the singularities of this bundle distributed ?

For fixed values $|\mu|$ and $\Im$ we get a level set of the momentum mapping $(|\mu|, \Im)$ : $T^*SO(3)\backslash SO(3) \longrightarrow \mathbb{R}^2$ to the 2-torus action

$$\mathsf{T} \times T^*SO(3)\backslash SO(3) \;\longrightarrow\; T^*SO(3)\backslash SO(3) \quad .$$

At regular values $(|\mu|, \Im)$ these level sets are 4-dimensional invariant manifolds of $X_{\bar{H}}$ , forming non-trivial $\mathsf{T}$-bundles with base spaces $S^2_{|\mu|} \times \{\Im\}$ . We can easily visualize this in *Figure 2.1.* The values of the momentum mapping are given by the common radius $|\mu|$ of the two spheres and by the height $\Im$ on the right hand sphere. Together the circle of height $\Im$ on the right hand sphere and the $S^1$-fibre form the $\mathsf{T}$-fibre of the 2-torus bundle, while the left hand sphere is the base space.

Hence, to perform the reconstruction we just have to attach a 2-torus to every point on the reduced phase space $S^2_{|\mu|} \times \{\Im\}$ . The equilibria correspond to invariant 2-tori, and the periodic orbits give rise to invariant 3-tori. The dynamics on these tori is conditionally periodic. The normal behaviour of the invariant 2-tori is induced from the linearisation of the corresponding equilibrium. We get normally elliptic as well as normally hyperbolic invariant 2-tori and occasionally normally parabolic invariant 2-tori.

The motion of the rigid body corresponding to such an invariant 2-torus is the same regular precession as in the Euler case. The angular momentum $\vec{\ell}$ remains fixed, as does the ratio $\frac{\Im}{|\mu|}$ . The figure axis $\vec{e}_3$ precesses around $\vec{\ell}$ and the body rotates about the figure axis. For an invariant 3-torus this rotational-precessional motion is superposed by a slow movement of the angular momentum $\vec{\ell}$ along the orbit of the reduced Hamilton function $\bar{H}_{|\mu|,\Im}$ . The same holds true for the motion reconstructed from the (un)stable manifolds of normally hyperbolic (or normally parabolic) invariant 2-tori.

When $\Im = \pm|\mu|$ the angular momentum $\vec{\ell}$ is parallel to the figure axis $\vec{e}_3$ and the 2-torus action degenerates. Indeed, the orbits of the action become circles $S^1$ , coinciding with the orbits of the central action. The level sets of the momentum mapping become $S^1$-bundles over $S^2_{|\mu|} \times \{\pm|\mu|\}$ and are diffeomorphic to $SO(3)$ . Hence, the periodic orbits of the reduced Hamiltonian vector field $X_{\bar{H}_{|\mu|,\pm|\mu|}}$ give rise to invariant 2-tori. However, these 2-tori are "not Eulerian". The body rotates around the angular momentum $\vec{\ell}$ which is parallel to the figure axis $\vec{e}_3$ , while $\vec{\ell}$ slowly moves along the orbit of the reduced Hamilton function $\bar{H}_{|\mu|,\pm|\mu|}$ . For invariant 3-tori the figure axis was not parallel to $\vec{\ell}$ , but precessed around $\vec{\ell}$ . Here we have the limit $\vec{e}_3 \to \vec{\ell}$ . In particular the invariant 2-tori are normally elliptic. From equilibria on $S^2_{|\mu|} \times \{\pm|\mu|\}$ we now reconstruct periodic orbits. The body rotates around the fixed angular momentum (which is parallel to the figure axis). Centres become elliptic periodic orbits, and saddles give rise to periodic orbits whose Floquet multipliers are one real pair and one complex conjugate pair on the unit circle. We call such a periodic orbit *hypoelliptic*, its normal behaviour is that of a saddle $\times$ a centre.

We also have to understand how the invariant level sets fit together to form the phase space $T^*SO(3)^{\backslash SO(3)}$ . We can collect the relevant information in one picture, the set of critical values of the energy-momentum mapping

$$\mathcal{EM} := (\bar{H}, |\mu|, \Im) : \quad T^*SO(3)^{\backslash SO(3)} \quad \longrightarrow \quad \mathbb{R}^3 \quad .$$

The regular values of $\mathcal{EM}$ just correspond to invariant 3-tori. The critical values correspond to normally elliptic 2-tori, to normally hyperbolic (or parabolic) 2-tori together with their (un)stable manifolds and to elliptic and hypoelliptic periodic orbits, the latter again together with their (un)stable manifolds. The critical values also mark the boundary of the image of the energy-momentum mapping. Since only the ratio $\frac{\Im}{|\mu|}$ is important we restrict to a slice of this set, fixing $|\mu|$ . *Figure 4.1* depicts one of the three generic cases. It depends on the mass distribution of the rigid body and on the parameters $(\alpha, \beta, \gamma, a, b, c)$ of the affine force field whether this or one of the other two cases applies. The critical values are symmetric with respect to the reflection $\Im \mapsto -\Im$ . The $|\mu|$-slice depicted in *Figure 4.1* consists of four curves, two of which have cusps. Let us describe how the phase portraits found in Section 3 are related to $\mathcal{EM}$ .

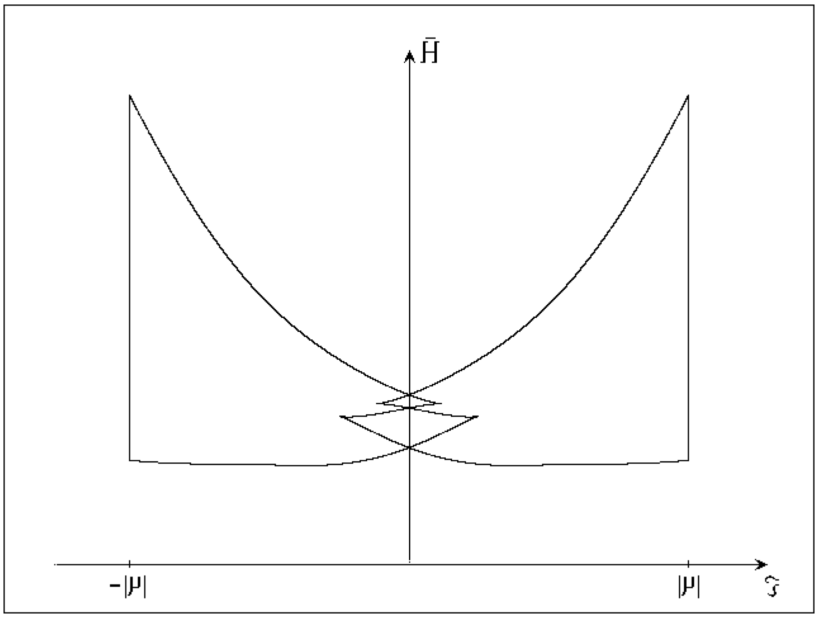


*Figure 4.1*: A $|\mu|$-slice of the set of critical values of the energy-momentum mapping $\mathcal{EM} = (\bar{H}, |\mu|, \Im)$ for $(\alpha, \beta, \gamma) \gg (a, b, c)$ .

For $\Im$ near $\pm\frac{|\mu|}{\sqrt{3}}$ there are two critical values $(h_1, |\mu|, \Im)$ and $(h_2, |\mu|, \Im)$ in every $|\mu|$-slice, confer *Figure 3.1.* They correspond to normally elliptic 2-tori. From the periodic orbits with energies $h$ between $h_1$ and $h_2$ we reconstruct invariant 3-tori, the values $(h, |\mu|, \Im)$ are regular. For energies $h$ outside the interval $[h_1, h_2]$ the ellipsoid $\{\bar{H}_{|\mu|,\Im} = h\}$ and the sphere $S^2_{|\mu|}$ do not intersect, $(h, |\mu|, \Im)$ is not in the image of $\mathcal{EM}$ . When the absolute value $|\Im|$ gets smaller, a *quasi-periodic centre-saddle bifurcation* generates another normally elliptic 2-torus and a normally hyperbolic invariant 2-torus, confer *Figure 3.2.* For $\Im$ near zero there is a second normally hyperbolic 2-torus and a fourth normally elliptic invariant 2-torus. The cusp points correspond to the normally parabolic invariant 2-tori where the quasi-periodic centre-saddle bifurcations take place. At $\Im = 0$ the two normally hyperbolic 2-tori have the same energy, confer *Figure 3.3.* The same holds true for the normally elliptic 2-tori, they come in pairs of the same energy. The values $(h, |\mu|, \pm|\mu|)$ are all critical. The values in the four "edges" of the image of the energy-momentum mapping ("corners" in the $|\mu|$-slice of *Figure 4.1*) correspond to elliptic periodic orbits.

What is different in the other generic cases ? If the linear part of the potential energy is sufficiently small compared to the quadratic part there also is a quasi-periodic centre-saddle bifurcation for some $\Im > \frac{|\mu|}{\sqrt{3}}$ (and symmetrically for the corresponding $\Im < -\frac{|\mu|}{\sqrt{3}}$ ). One can even have a second quasi-periodic centre-saddle bifurcation for $|\Im|$ in $]\frac{|\mu|}{\sqrt{3}}, |\mu|[$ for appropriate values of $\alpha, \beta, \gamma$ and $a, b, c$ . In these cases the normally elliptic and hyperbolic 2-tori born in such bifurcations shrink to periodic orbits when $\Im \longrightarrow \pm|\mu|$ . As in the four "edges" of the image of the energy-momentum mapping, the normally elliptic 2-tori shrink down to elliptic periodic orbits. The normally hyperbolic 2-tori shrink to hypoelliptic periodic orbits.

We use the polynomials $f_i$ introduced in the proof of Theorem 3.1 to define the functions

$$\begin{aligned} e_1^\delta(\lambda) &:= \tfrac{-s_3}{I_3-I_1} + \delta\sqrt{\tfrac{s_3^2}{(I_3-I_1)^2} + 12\tfrac{(f_5(\lambda))^2}{f_2(\lambda)}} \\ e_2^\delta(\lambda) &:= \tfrac{e_1^\delta(\lambda)\sqrt{f_2(\lambda)}}{6\, f_5(\lambda)} \\ e_3^\delta(\lambda, |\mu|) &:= \tfrac{|\mu|^2}{2I_1} - \tfrac{I_3-I_1}{I_1 I_3}\tfrac{(e_2^\delta(\lambda))^2|\mu|^2}{2} \\ &\quad + \tfrac{a+b+c}{2}(I_1 + (I_3-I_1)(e_2^\delta(\lambda))^2) + s_3\tfrac{f_6(\lambda)\, e_1^\delta(\lambda)}{(f_5(\lambda))^2} \end{aligned} \tag{4}$$

which are needed for the description of the set of critical values to which we turn now.

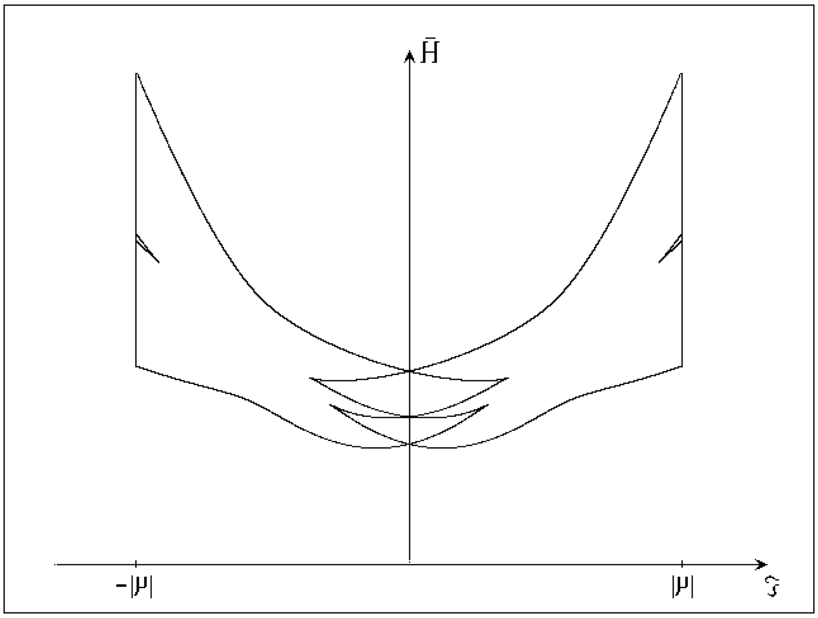


*Figure 4.2*: The $|\mu|$-slice of $\Sigma$ for $(\alpha, \beta, \gamma) \approx (a, b, c)$ .

*Theorem 4.1*

*Let* $\bar{H} : T^*SO(3)\backslash SO(3) \longrightarrow \mathbb{R}$ *denote the Hamilton function (1). The set* $\Sigma \subseteq \mathbb{R}^3$ *of critical values of the energy-momentum mapping* $\mathcal{EM} = (\bar{H}, |\mu|, \Im)$ *is symmetric with respect to the reflection* $\Im \mapsto -\Im$ *in the third component. For external parameters* $\alpha, \beta, \gamma, a, b, c$ *in general position this set has, at fixed values of* $|\mu|$ *, one of the three forms shown in Figures 4.1–4.3.*

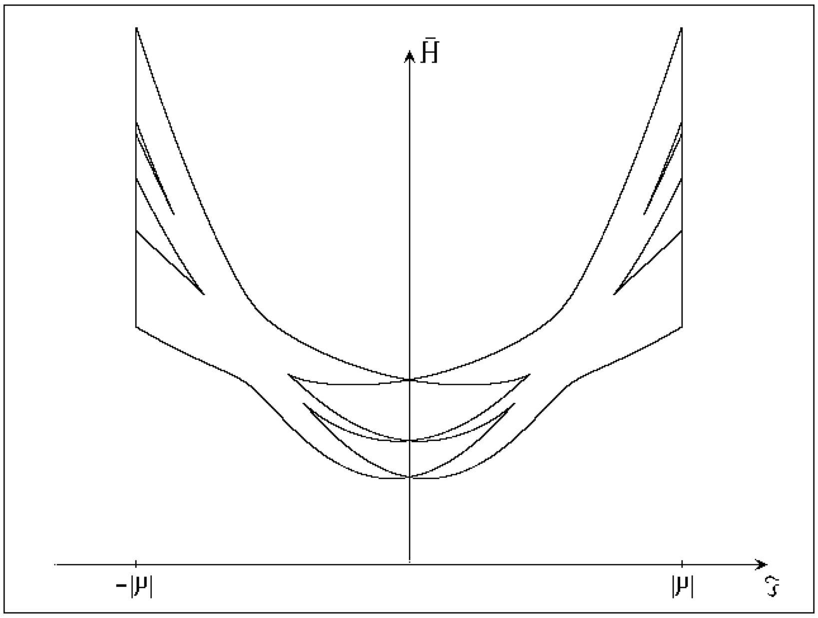


*Figure 4.3*: The $|\mu|$-slice of $\Sigma$ for $(\alpha, \beta, \gamma) \ll (a, b, c)$ .

*The regular points of* $\Sigma$ *stand for normally elliptic and (on the arcs extending between the cusp points) normally hyperbolic invariant 2-tori (together with their stable and unstable manifolds). The cusp points of* $\Sigma$ *correspond to normally parabolic invariant 2-tori, here a quasi-periodic centre-saddle bifurcation takes place. For intersection points at* $\Im = 0$ *the corresponding invariant 2-tori have the same energy and the hyperbolic ones are connected by heteroclinic orbits. The intersection points at* $\Im = \pm|\mu|$ *correspond to periodic orbits.*

*The* $\bar{H}$*-component of* $\Sigma$ *depends in a quadratic way on* $|\mu|$ *, while distances on* $\Sigma$ *in the* $\bar{H}$*-direction are independent of* $|\mu|$ *. Distances in the* $\Im$*-direction increase linearly with* $|\mu|$ *. Taking the direction perpendicular to the plane of drawing as the* $|\mu|$*-axis,* $\Sigma$ *is a paraboloid growing out of Figure 4.1, 4.2 or 4.3, respectively. In particular a level set of* $\Sigma$ *with constant value of the energy* $\bar{H}$ *is diffeomorphic to a* $|\mu|$*-slice.*

*To be more precise,* $\Sigma = \Sigma_+ \cup \Sigma_- \cup \Sigma_l \cup \Sigma_r$ *is the union of four surfaces that allow the following parametrisations :*

$$\begin{aligned}
\Sigma_+ &= \{ \, ( e_3^\delta(\lambda, |\mu|), |\mu|, \epsilon\, e_2^\delta(\lambda)\, |\mu| \,) \in \mathbb{R}^3 \;\big|\; \lambda \in \Lambda_{|\mu|}^{\delta,+} \, , \, |\mu| > 0 \, , \, \epsilon\cdot\delta = 1 \, \} \\
\Sigma_- &= \{ \, ( e_3^\delta(\lambda, |\mu|), |\mu|, \epsilon\, e_2^\delta(\lambda)\, |\mu| \,) \in \mathbb{R}^3 \;\big|\; \lambda \in \Lambda_{|\mu|}^{\delta,-} \, , \, |\mu| > 0 \, , \, \epsilon\cdot\delta = -1 \, \}
\end{aligned}$$

$$\begin{array}{rcl} \Sigma_l & = & \{\ (\lambda, |\mu|, -|\mu|) \in \mathbb{R}^3 \ \big|\ \lambda \in \Lambda_{|\mu|}\ ,\ |\mu| > 0\ \} \\ \Sigma_r & = & \{\ (\lambda, |\mu|, |\mu|) \in \mathbb{R}^3 \ \big|\ \lambda \in \Lambda_{|\mu|}\ ,\ |\mu| > 0\ \} \end{array} \quad .$$

*Here $\epsilon, \delta = \pm 1$ and the $e_i^{\pm}$ are given by (4). The three possible cases are distinguished by the number of solutions of the two equations $e_2^{\sigma}(\lambda) = -\sigma$ and $e_2^{\sigma}(\lambda) = \sigma$ , where $\sigma = -\mathrm{sgn}(\frac{s_3}{I_3 - I_1})$ ; these solutions correspond to the intersection points at $\Im = \pm|\mu|$ . Denoting these solutions by $\lambda_1 < a < \lambda_3 < \lambda_4 < b < \lambda_5 < \lambda_6 < c < \lambda_2$ (with possibly $\lambda_3, \lambda_4$ and/or $\lambda_5, \lambda_6$ not existing) we have*

$$\begin{array}{rcccl} & & \Lambda_{|\mu|} & = & [\, e_3^{\sigma}(\lambda_1, |\mu|)\,,\, e_3^{\sigma}(\lambda_2, |\mu|)\,] \\ \Lambda_{|\mu|}^{\sigma,+} & = & \Lambda_{|\mu|}^{\sigma,-} & = & ]-\infty, \lambda_1] \cup [\lambda_3, \lambda_4] \cup [\lambda_5, \lambda_6] \cup [\lambda_2, \infty[ \\ \Lambda_{|\mu|}^{-\sigma,+} & = & \Lambda_{|\mu|}^{-\sigma,-} & = & \mathbb{R} \quad . \end{array}$$

Proof :

The reflectional symmetry $\Im \mapsto -\Im$ of $\mathrm{im}\,\mathcal{EM}$ is induced by the symmetry $\alpha \mapsto -\alpha$ of $T^*SO(3)^{\backslash SO(3)}$ (which leaves $\bar{H}$ and $|\mu|$ invariant). The genericity conditions we impose on $\alpha, \beta, \gamma, a, b, c$ are $\alpha \cdot \beta \cdot \gamma \neq 0$ , $a \neq b \neq c \neq a$ and $e_2^{\sigma}(\lambda_-) \neq \sigma$ , $e_2^{\sigma}(\lambda_+) \neq -\sigma$ , where $\sigma = -\mathrm{sgn}(\frac{s_3}{I_3 - I_1})$ and $\lambda_{\pm}$ are the two real roots of the polynomial $f_3$ , confer the proof of Theorem 3.1. The set of $(\alpha, \beta, \gamma, a, b, c)$ that satisfy these conditions is open and dense in $\mathbb{R}^6$ . The Galois group of $f_3$ being $\mathcal{S}_6$ , the permutation group of six elements, the last two conditions cannot be made explicit. However, once $\alpha, \beta, \gamma, a, b, c$ are given it is straightforward to check all the conditions. Upon the replacement $(a, b, c) \mapsto (a+d, b+d, c+d)$ , *i.e.* adding $\frac{I_1 + I_1 + I_3}{2} d$ to $\bar{H}$ , and relabelling $\vec{e}_x, \vec{e}_y, \vec{e}_z$ , we may assume $0 < a < b < c$ . Furthermore we use the reflections $\mu_i \mapsto -\mu_i$ to ensure $\alpha, \beta, \gamma > 0$ .

The two surfaces $\Sigma_l$ and $\Sigma_r$ consist of the values $\mathcal{EM}$ takes in the points where the functions $|\mu|$ and $\Im$ have parallel derivatives. It remains to show how the two curves $(\mathcal{I}^{\pm}(\lambda), h(\lambda))$ encountered in the proof of Theorem 3.1 lead to $\Sigma_+ \cup \Sigma_-$ . We have to invert the relation between $\mathcal{I}$ and $\Im$ , see *Figure 4.4*, and translate our results back to

$$\Im \;=\; \frac{|\mu|}{6\mathcal{I}}\Big( \frac{-s_3}{I_3 - I_1} + \delta \sqrt{\frac{s_3^2}{(I_3 - I_2)^2} + 12\mathcal{I}^2}\ \Big) \quad , \ \delta = \pm 1 \quad .$$

Recall that multiplying $\mathcal{H}_{\mathcal{I}}$ by $(I_3 - I_1)\frac{|\mu|^2 - 3\Im^2}{|\mu|^2} \stackrel{!}{=} \frac{s_3 \Im}{\mathcal{I}|\mu|}$ yields the two last terms of (1). Still neglecting the first three terms of (1), the two curves $(\mathcal{I}^{\epsilon}(\lambda), h(\lambda))$ , $\epsilon = \pm 1$ , give rise to

$$(\Im^{\epsilon,\delta}(\lambda), h^{\delta}(\lambda)) \;=\; \Big( \frac{\epsilon \sqrt{f_2(\lambda)}\,|\mu|}{6\, f_5(\lambda)} e_1^{\delta}(\lambda)\,,\ \frac{s_3\, f_6(\lambda)}{6\,(f_5(\lambda))^2} e_1^{\delta}(\lambda) \Big) \quad .$$

The union of the two curves with $\epsilon \cdot \delta = 1$ is connected, the same holds for the union of the two curves with $\epsilon \cdot \delta = -1$ . Indeed, $\lim_{\lambda \to \pm\infty} (\Im^{\epsilon,\delta}(\lambda), h^{\delta}(\lambda)) = \frac{\pm\delta}{\sqrt{3}}(\epsilon|\mu|, s_3\sqrt{\alpha^2 + \beta^2 + \gamma^2})$ .

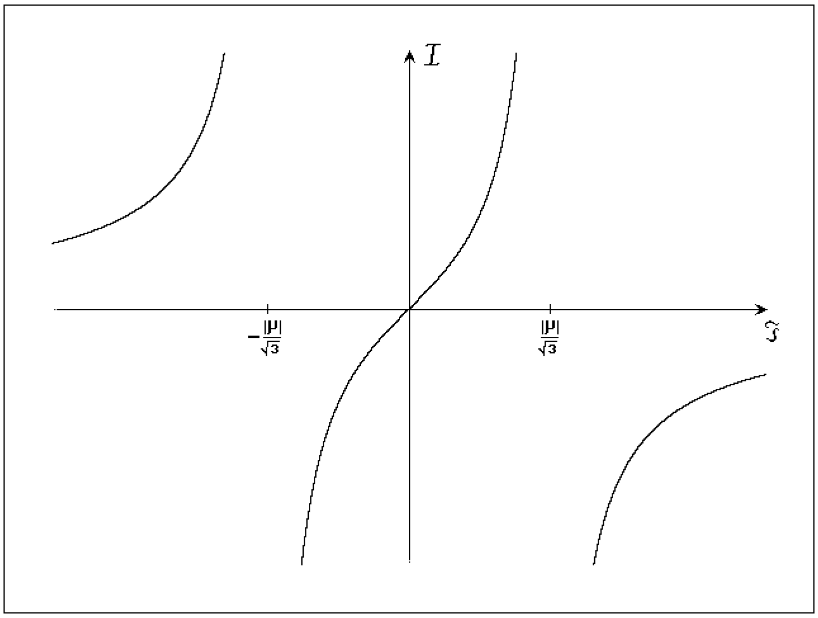


*Figure 4.4*: The relation between $\Im$ and $\mathcal{I}$ .

Parametrising the critical values near $\Im = \pm\frac{|\mu|}{\sqrt{3}}$ by $\Im$ we see that these curves are smoothly connected.

The possible $\Im^{\epsilon,\sigma}(\lambda)$ with $\sigma = -\mathrm{sgn}(\frac{s_3}{I_3-I_1})$ are restricted by the condition $|\Im| \le |\mu|$ . This excludes the parameters with $|\Im^{\epsilon,\sigma}(\lambda)| > |\mu|$ from the domain of $\lambda$ . In particular we have three possible cases according to whether none, one or both of $\Im^{-\tau,\sigma}(\lambda_\tau)$ , $\tau = \pm 1$ , are smaller than $|\mu|$ ; we do not distinguish between $\Im^{+,\sigma}(\lambda_-) < |\mu| < \Im^{-,\sigma}(\lambda_+)$ and $\Im^{+,\sigma}(\lambda_-) > |\mu| > \Im^{-,\sigma}(\lambda_+)$ . The cases where a cusp point lies on $\Im = \pm|\mu|$ are excluded by the genericity condition $e_2^\sigma(\lambda_\tau) \ne -\sigma\tau$ . The equation $e_2^\sigma(\lambda) = -\sigma$ always has a solution $\lambda_1 < a$ , and in case $|e_2^\sigma(\lambda_+)| < 1$ there are two more solutions $\lambda_5, \lambda_6 \in ]b, c[$ . Dually, the equation $e_2^\sigma(\lambda) = \sigma$ always has a solution $\lambda_2 > c$ , and in case $|e_2^\sigma(\lambda_-)| < 1$ there are two more solutions $\lambda_3, \lambda_4 \in ]a, b[$ . These parameter values correspond to periodic orbits on $T^*SO(3)\backslash SO(3)$ .

Finally we add the first three terms of (1) to $h^\delta(\lambda)$ . The second and third term $\frac{a+b+c}{2}I_1 + \frac{I_3-I_1}{2}(a+b+c-\frac{|\mu|^2}{I_1 I_3})(e_2^\delta(\lambda))^2$ alter the tangents at the cusp points in the $|\mu|$-slice. For sufficiently large $|\mu|$ both cusps point upwards (or downwards, depending on the sign of $I_3 - I_1$ ). For small $|\mu|$ one or both cusps might point in the other direction, correspondingly there is an intermediate value of $|\mu|$ where the cusp has a horizontal tangent. The first term $\frac{|\mu|^2}{2I_1}$ in (1) arranges the $|\mu|$-slice sets of $\Sigma$ in a parabolic way along the $|\mu|$-axis ; **q.e.d.**

Our description of the averaged flow and the related one-degree-of-freedom systems relies on the genericity conditions $I_1 \neq I_3$ , $s_3 \neq 0$ , $\alpha \cdot \beta \cdot \gamma \neq 0$ and $a \neq b \neq c \neq a$ . If these are not fulfilled, higher order normal forms might be needed. For instance, the case $s_3 = 0$ requires a normal form of order 2 to break the discrete symmetries which are present in the normal form of order 1 in this case, but not in the original system. On the other hand, if the original system itself admits (discrete) symmetries one should resort to equivariant singularity theory when studying the normal form. To fix thoughts consider the case $a < b < c$ with $\alpha = 0 = \gamma$ and $\beta \neq 0$ where the Hamilton function is $\mathbb{Z}_2 \times \mathbb{Z}_2$-symmetric. Here the normally elliptic and normally hyperbolic invariant 2-tori do not meet in quasi-periodic centre-saddle bifurcations, but in *quasi-periodic Hamiltonian pitchfork bifurcations*. This is studied in [Hanßmann;96], where the program formulated in Section 2 is applied to this $\mathbb{Z}_2 \times \mathbb{Z}_2$-symmetric case.

In Theorem 4.1 we excluded the values of $(\alpha, \beta, \gamma, a, b, c)$ for which there are *para-elliptic* periodic orbits at $\Im = \pm|\mu|$ , *i.e.* where the normal linear behaviour is that of a parabolic equilibrium $\times$ a centre. These para-elliptic periodic orbits would not be isolated, but form a 1-parameter family which is not a robust situation. Nevertheless, it would be instructive to study how the family unfolds within $X_H$ . Here one might also use $(\alpha, \beta, \gamma, a, b, c)$ as unfolding parameters. These external parameters should not be mixed with the internal or distinguished parameters $|\mu|$ and $\Im$ . In [Broer,Chow,Kim,Vegter;93] the 'generic' case of isolated para-elliptic equilibria is treated in this fashion.

## Conclusion

In the previous section we could give a quite detailed description of the dynamics of $\bar{H}$ on $T^*SO(3)^{\backslash SO(3)}$ . This is due to the 2-torus symmetry. The behaviour is governed by the reduced system with one degree of freedom. But unlike these one-degree-of-freedom systems the vector field $X_{\bar{H}}$ is not structurally stable (in the class of Hamiltonian vector fields on $T^*SO(3)^{\backslash SO(3)}$ ). Under any small perturbation it can (and usually does) lose its integrability. We will study the implications for the original system $X_H$ more thoroughly in the sequel [Hanßmann;97] to this paper, see also [Hanßmann;95b]. Here we give a short account on the methods and results.

We have to keep track of several perturbation problems here. First, our "original Hamilton function" $H$ is a perturbation (of order $\varepsilon$ ) of the free rigid body with kinetic energy $T$ . Using Theorem 2.1 we consider $H$ as a perturbation (of order $\varepsilon^2$ ) of its normal form $\bar{H}$ . Furthermore we know that perturbations of the family $\bar{H}_{|\mu|,\Im}$ of one-degree-of-freedom systems do not lead to qualitative changes. This is what we want to use to gain information about the perturbation from $\bar{H}$ to $H$ . Ordinary KAM-theory tells us that diophantine 3-tori survive as a Cantor family of large measure, confer [Arnol'd;63b], [Pöschel;82] and [Mazzocco;97].

The structural stability of the one-degree-of-freedom systems concerns the Eulerian 2-tori. Indeed, the periodic orbits on $S^2_{|\mu|} \times \{\Im\}$ do not tell us whether the family $X_{\bar{H}_{|\mu|,\Im}}$ is structurally stable ; this question is decided by the behaviour of the equilibria. These equilibria give rise to invariant 2-tori on $T^*SO(3)\backslash SO(3)$ , they are the Eulerian 2-tori that survive the perturbation from $T$ to $\bar{H} = T + \bar{V}$ . The $X_{\bar{H}}$-invariant 2-tori are normally hyperbolic or normally elliptic, occasionally such families meet and vanish in a quasi-periodic centre-saddle bifurcation. For the persistence of (Cantor families of) normally hyperbolic and normally elliptic 2-tori we use the generalization of KAM-theory presented in [Moser;67], [Graff;74] and [Broer,Huitema,Takens;90], see also [Broer,Huitema,Sevryuk;96] and references therein. The Eulerian 2-tori that survive the perturbation $H$ of $T$ form Cantor families which are close to the Eulerian 2-tori of the averaged system $X_{\bar{H}}$ .

For our three-step program to work it is essential that the normal form defines an integrable system. When working with a "minimally" superintegrable system like the Euler top this is immediate. On the other hand, if the superintegrable system has, *e.g.*, $n+2$ integrals, then the normal form of a given perturbation leads to a reduced system with two degrees of freedom. Generically this reduced system is non-integrable. Thus global information on small perturbations of such a superintegrable system is not available (unless the perturbation is of a very special kind, "removing the degeneracy"). Still, one might find centres or elliptic periodic orbits of the reduced system and conclude the existence of "many" invariant $n$-tori in the original system. This is used in [Arnol'd;63b] to show that "most" planets with small eccentricity and inclination do not leave the solar system (nor collide).

Hamiltonian systems behave in the neighbourhood of an equilibrium like a perturbation of an integrable system. If there are no resonances among the (normal) frequencies of the equilibrium, the Birkhoff series defines a nondegenerate integrable approximation. For "higher order resonances" the same holds true for a suitable Birkhoff polynomial, confer [Sanders;77]. The case of a single resonance of order 3 or 4 is studied in [Kummer;90]. Here the Birkhoff normalizing transformation leads to a normal form "with a resonance term" that allows again the reduction to a one-degree-of-freedom system.

## Bibliography

*R. Abraham, J.E. Marsden* [78] *Foundations of Mechanics*, 2nd ed.; Benjamin (1978)

*M.H. Andoyer* [23] *Cours de Mécanique Celeste* ; Gauthier-Villars (1923,1926)

*V.I. Arnol'd* [63a] Proof of a theorem of A. N. Kolmogorov on the invariance of quasi-periodic motions under small perturbations of the Hamiltonian ; *Russ. Math. Surv.* **18**(5), p. 9 – 36 (1963)

*V.I. Arnol'd* [63b] Small denominators and problems of stability of motion in classical and celestial mechanics ; *Russ. Math. Surv.* **18**(6), p. 85 – 191 (1963)

*V.I. Arnol'd, V.V. Kozlov, A.I. Neishtadt* [85] Mathematical Aspects of Classical and Celestial Mechanics ; in *Dynamical Systems III* (ed. V.I. Arnol'd) Springer (1988)

*G. Benettin, F. Fassò* [96] Fast rotations of the rigid body : a study by Hamiltonian perturbation theory. Part I ; *Nonlinearity* **9**, p. 137 – 186 (1996)

*G. Benettin, F. Fassò, M. Guzzo* [97] Fast Rotations of the Rigid Body : A Study by Hamiltonian Perturbation Theory. Part II : Gyroscopic Rotations ; preprint, University of Padova (1997)

*H.W. Broer, S.-N. Chow, Y. Kim, G. Vegter* [93] A normally elliptic Hamiltonian bifurcation ; *Z. angew. Math. Phys.* **44**, p. 389 – 432 (1993)

*H.W. Broer, G.B. Huitema, M.B. Sevryuk* [96] *Quasi-Periodic Motions in Families of Dynamical Systems : Order amidst Chaos* ; LNM **1645**, Springer (1996)

*H.W. Broer, G.B. Huitema, F. Takens* [90] Unfoldings of quasi-periodic tori ; *Mem. AMS* **83** #421, p. 1 – 82 (1990)

*R. Cushman, L. Bates* [97] *Global Aspects of Classical Integrable Systems* ; Birkhäuser (1997)

*A. Deprit* [67] Free Rotation of a Rigid Body Studied in the Phase Plane ; *Am. J. Phys.* **35**, p. 424 – 428 (1967)

*A. Elipe, H. Hanßmann* [97] The bifurcation diagram of the family of quadratic Hamiltonians on the sphere, with applications to gyrostats with two or three rotors — *in preparation*

*F. Fassò* [91] *Fast rotations of the rigid body and Hamiltonian perturbation theory* ; Ph.D. thesis, SISSA, Trieste (1991)

*F. Fassò* [94] Perturbation theory for systems without global action-angle coordinates ; p. 213 – 220 in *Hamiltonian Mechanics : Integrability and Chaotic Behaviour, Torun 1993* (ed. J. Seimenis) Plenum (1994)

*F. Fassò* [95] Hamiltonian perturbation theory on a manifold ; *Celest. Mech. Dyn. Astr.* **62**, p. 43 – 69 (1995)

*F. Fassò* [96] The Euler-Poinsot top : A non-commutatively integrable system without global action-angle coordinates ; *Z. angew. Math. Phys.* **47**, p. 953 – 976 (1996)

*S.M. Graff* [74] On the Conservation of Hyperbolic Invariant Tori for Hamiltonian Systems ; *J. Diff. Eq.* **15**, p. 1 – 69 (1974)

*H. Hanßmann* [95a] Normal Forms for Perturbations of the Euler Top ; p. 151 – 173 in *Normal Forms and Homoclinic Chaos, Waterloo 1992* (eds. W.F. Langford, W. Nagata) Fields Institute Communications **4** (1995)

*H. Hanßmann* [95b] *Quasi-periodic Motions of a Rigid Body — A case study on perturbations of superintegrable systems* ; Ph.D. thesis, Rijksuniversiteit Groningen (1995)

*H. Hanßmann* [96] Equivariant Perturbations of the Euler Top ; p. 227 – 253 in *Nonlinear Dynamical Systems and Chaos, Groningen 1995* (eds. H.W. Broer et al.) Birkhäuser (1996)

*H. Hanßmann* [97] Quasi-periodic Motions of a Rigid Body II : Implications for the Original System — *in preparation*

*M. Kummer* [90] On Resonant Classical Hamiltonians with $n$ Frequencies ; *J. Diff. Eq.* **83**, p. 220 – 243 (1990)

*V. Lanchares, A. Elipe* [95a] Bifurcations in biparametric quadratic potentials ; *Chaos* **5**(2), p. 367 – 373 (1995)

*V. Lanchares, A. Elipe* [95b] Bifurcations in biparametric quadratic potentials. II ; *Chaos* **5**(3), p. 531 – 535 (1995)

*V. Lanchares, M. Iñarrea, J.P. Salas, J.D. Sierra, A. Elipe* [95] Surfaces of bifurcation in a triparametric quadratic Hamiltonian ; *Phys. Rev. E* **52**(5), p. 5540 – 5548 (1995)

*P. Libermann, C.-M. Marle* [86] *Symplectic Geometry and Analytical Mechanics* ; D. Reidel (1987)

*M. Mazzocco* [97] KAM theorem for generic analytic perturbations of the Euler system ; *Z. angew. Math. Phys.* **48**, p. 193 – 219 (1997)

*J. Moser* [67] Convergent Series Expansion for Quasi-Periodic Motions ; *Math. Ann.* **169**(1), p. 136 – 176 (1967)

*J. Pöschel* [82] Integrability of Hamiltonian Systems on Cantor Sets ; *Comm. Pure Appl. Math.* **35**, p. 653 – 696 (1982)

*R.A. Posthumus, J. Scholtmeijer* [90] *Chaos and Fractals. Practicumhandleiding bij* DYNPAO ; Rijksuniversiteit Groningen (1990)

*J. Sanders* [77] Are higher order resonances really interesting ? *Celest. Mech.* **16**, p. 421 – 440 (1978)

*S. Wolfram* [88] *Mathematica : A System for Doing Mathematics by Computer* ; Addison-Wesley (1988)

Heinz Hanßmann
Institut f. Reine & Angewandte Mathematik
RWTH Aachen
52056 Aachen
Germany
email : Heinz@iram.rwth-aachen.de